**Solid Freeform Fabrication 2023: Proceedings of the 34th Annual International Solid Freeform Fabrication Symposium – An Additive Manufacturing Conference**
**Reviewed Paper**

# Fatigue Life Prediction of Functionally Graded TPU and PLA Components Produced by Material Extrusion

Suhas Alkunte[1], Mithila Rajeshirke[1], Orkhan Huseynov[1], Dr. Ismail Fidan [2]
[1]Department of Mechanical Engineering, Tennessee Tech University, Cookeville, TN 38505, USA
[2]Department of Manufacturing and Engineering Technology, Tennessee Tech University, Cookeville, TN 38505, USA

## Abstract

The objective of the present research is to examine the fatigue life estimation of functionally graded additive manufacturing (FGAM) components produced by the Material Extrusion (MEX). Current research studies demonstrate the potential of functionally graded materials (FGMs) in enhancing the mechanical properties of engineered structures. The raw materials employed for the experimentation of this study are a combination of Polylactic acid (PLA) and Thermoplastic Polyurethane (TPU). To predict fatigue life, several researchers have utilized various statistical approaches. In this investigation, an experimental study is conducted utilizing Tension-Tension (T-T) loading conditions and different stress levels (80, 60, 40, and 20% of Ultimate tensile strength), followed by the application of Basquin's Model for fatigue life prediction. The results obtained indicate that the model may be utilized to predict fatigue response. Overall, the soft-hard material combinations with adaptable properties produced through FGAM have potential applications in dental and orthopedic fields.

**Keywords**: Fatigue life; Fatigue Prediction; Basquin's Model; S-N Curve; FGAM

## Introduction

Multi-material additive manufacturing (MMAM) has engrossed numerous researchers due to its inherent advantages. MMAM facilitates the fabrication of parts encompassing diverse materials in a single manufacturing process, wherein these materials can exhibit distinct chemical, physical, mechanical, and electrical properties [1]. In the last twenty years, AM has emerged as a pivotal technology within the manufacturing industry. AM technologies have revolutionized traditional manufacturing methods by offering several significant advantages [2]. Compared to conventional approaches, AM eliminates the requirement for extensive tooling [3], resulting in cost and time savings [4]. Additionally, AM provides unparalleled flexibility in design and allows for easy modification of products during the manufacturing process. These capabilities empower manufacturers to rapidly iterate and customize designs, leading to improved efficiency and innovation in the production of various components and products [5]. MMAM encompasses a comprehensive classification comprising seven distinct technologies. These include material extrusion, vat photopolymerization, powder bed fusion, material jetting, direct energy deposition, sheet lamination, binder jetting, and hybrid additive manufacturing [6]. Each technology offers unique capabilities and characteristics, contributing to the versatility and potential of MMAM in achieving precise material combinations and complex part geometries [7]. The MEX process in MMAM, a variety of materials are utilized, including thermoplastics, metal-filled thermoplastics, composites, and more. Figure 1 provides a schematic view depicting the process description of the MEX process in MMAM.

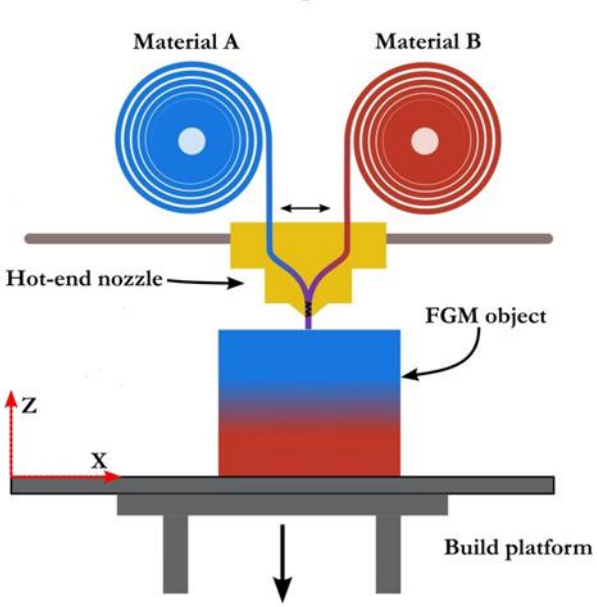


*Figure 1: Process description of MEX process* [8]

FGMs represent cutting-edge composite materials that exhibit gradual variation in constituent composition and/or microstructure along specific directions [9]. This unique characteristic distinguishes FGMs from traditionally manufactured laminated composites and offers a significant advantage. The smooth and continuous variation in material properties within FGMs mitigates the occurrence of debonding and delamination failures commonly associated with laminates [10]. The customized nature of FGMs allows for the attainment of superior qualities in thermal conductivity, hardness, mechanical strength, and electrical conductivity. By tailoring the material properties to specific requirements, FGMs enable enhanced performance and durability in a wide range of applications [11]. FGMs can be produced using various manufacturing technologies, but AM presents a compelling opportunity to address the limitations of conventional manufacturing processes for composite materials. AM enables the simultaneous deposition of multiple materials in pre-defined ratios, resulting in a controlled variation of composition and microstructure across different regions of the fabricated component. This ability to customize material characteristics in specific areas offers a significant advantage in tailoring the properties of FGMs according to desired specifications. By leveraging AM, manufacturers can achieve precise control over material composition, enabling the creation of complex and highly functional components with enhanced performance and unique material characteristics [10]–[12].Thermoplastic materials exhibit inherent anisotropic characteristics [13]. For several decades, the S-N behavior has been fundamental in the analysis of material fatigue life, tracing its roots back to the nineteenth century [14]. Characterizing the S-N curve holds great importance not only for engineering materials but also for accurately predicting the fatigue life of various components under cyclic loads. However, the prediction of fatigue life remains a challenging task due to the complex nature of fatigue mechanisms and the numerous factors that influence the fatigue behavior of materials and structures [15]. Furthermore, thermoplastics exhibits a wide range of damage mechanisms. In the case of composite materials, their fatigue behavior differs significantly from isotropic materials like metals. Micro-cracks in composites can initiate at an early stage of loading, yet the materials can still endure the load until ultimate failure occurs. However, to establish fatigue S-N curves, ASTM, and ISO standards [16] define experimental parameters and procedures that involve testing

multiple samples. Moreover, to minimize costs in terms of time and resources, it is crucial to explore statistical methods for curve fitting. Various models, such as Basquin's model [17], the Weibull distribution approach [18], the Coffin-Manson relation [19], and advanced statistical analyses like artificial neural networks (ANN) [20] , have been successfully employed to predict and fit the fatigue behavior of diverse materials. Another one-of-a-kind study was conducted by Eskandari et al. [19] proposed a framework for validating a fatigue damage function and developed a theory for predicting the remaining fatigue life at different stress levels with a constant stress ratio. They experimentally validated the theory, focusing solely on the zero-stress condition. Later, Pertuz et al. [21] investigated the effects of various parameters, including fiber-reinforcing materials (fiberglass, Kevlar, and carbon fiber), infill pattern (triangular and hexagonal), infill orientation (0°, 45°, and 60°), and concentric ring reinforcements. The researchers utilized Basquin's model for predicting fatigue life due to its simplicity. They established a logarithmic relationship between stress (S) and cycles to failure (Nf) for loading conditions corresponding to 95%, 90%, 85%, and 80% of the ultimate tensile stress. To analyze the obtained data at each load level, the Weibull distribution was selected as the statistical method for data adjustment. Another one-of-a-kind study conducted by Burhan et al. [13] employed several statistical models to predict fatigue life in the study. The analysis included a broad range of stress ratios, with a focus on reviewing and analyzing S-N curve models. The findings revealed that the models developed specifically for characterizing fatigue data demonstrated significantly better data fitting capabilities compared to the models designed to forecast the impact of stress ratios. Additionally, Marino et al. [22] focused on examining the fatigue properties of different polymer materials. The experimental data was validated using the mathematical Basquin's model. Specifically, the research work highlighted the rotating bending fatigue data obtained from 3D printed specimens fabricated using the specified materials. The specimens were subjected to various loading conditions for the purpose of analysis. Similarly, Ghods et al. [23] conducted fatigue life study on Grade 5 Ti6Al4V fabricated through electron beam powder bed fusion. The study investigated the influence of various build and component design parameters on fatigue performance. The fatigue responses were used to construct stress-life diagrams, and the data was fitted to Basquin's model. The stress-life distributions were then statistically analyzed using multiple linear regression to evaluate their relationship with the factors under consideration. Eventually, Mu et al. [24] introduced a novel S-N model, to elucidate the relationships between loads and fatigue life in the context of cyclic loading with constant amplitude. This model offers the ability to assess the fatigue life behavior of fiber reinforced plastic composites under various loading conditions, including tension-tension, tension-compression, or compression-compression loading, encompassing a range of fatigue life stress ratios. Pertuz et al. [21] conducted fatigue bending tests on continuous fiber-reinforced composites fabricated using the MEX technique under different loading conditions. The composites consisted of Onyx as the matrix material with 19% continuous Kevlar fiber reinforcement. The experimental data obtained from the tests were fitted to Basquin's model, which accurately represented 95.2% of the experimental data. Analysis of the parameter "b" in Basquin's equation indicates that the composite exhibits brittle behavior. Finally, Fard et al.[25] performed fatigue tests on samples, both with and without notches, utilizing a load ratio of 0.1. The experimental results were then compared to predictions. The findings indicated that the fatigue strength reduction factors and fatigue lifetimes were notably influenced by the raster orientation parameter. To date, no published studies have focused on predicting the fatigue behavior of FGMs produced using MMAM. Thus, the objective of this paper is to validate the experimental fatigue data using Basquin's model. A statistical model is employed to forecast the fatigue life of FGM

components manufactured using TPU and PLA. The experimental data is utilized to determine the coefficients of Basquin's model and predict the fatigue behavior. Subsequently, the predicted values by Basquin's model are benchmarked against the remaining experimental data. The research work makes a unique contribution through the design, manufacturing, and characterization of additively manufactured components using the MMAM process. Figure 2 illustrates the process for obtaining fatigue life predictions for FGM test samples. The specimen preparation precedes the tensile and fatigue testing, and the generated experimental data is then employed for fatigue life prediction.

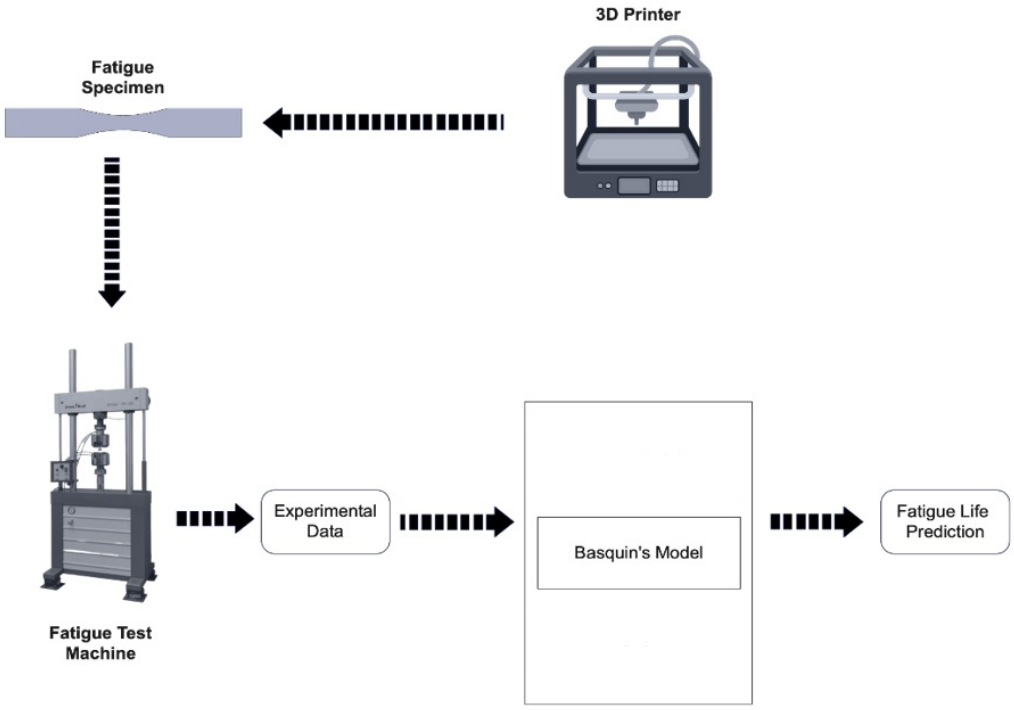


*Figure 2: Flowchart for statistical analysis of fatigue life prediction*

## Materials and Methods

The present study employed amorphous polymers such as TPU and PLA. These polymers were obtained commercially in filament form from the Push Plastic company. Table 1 presents the parameters that were utilized to 3D print the specimens in the investigation.

*Table 1: Fixed processing parameters*

| **Parameters** | **Values** |
|---|---|
| Nozzle temperature ($^{o}$C) | 210 |
| Bed temperature ($^{o}$C) | 60 |
| Infill density (%) | 100 |
| Infill pattern | Line (0/90) |

| | |
|---|---|
| Layer width (mm) | 0.35 |
| Layer height (mm) | 0.2 |
| Printing speed (mm/sec) | 15 |

TPU exhibits excellent flexibility throughout a wide range of hardness levels, making it highly versatile. It possesses exceptional low-temperature performance and impact strength. TPU also demonstrates excellent resistance to abrasion, oil, and grease. The ideal conditions for printing TPU specimens such as bed temperature, nozzle temperature, printing speed are 60°C, 220°C, and 15 mm/s are recommended [11]. Notably, it is crucial to disable retraction settings for optimal results. TPU finds extensive applications across various industries, including automotive[26], aerospace, mobile coverings, medical equipment, and wire and cable manufacturing, owing to its unique combination of plastic and rubber properties [27]. PLA is a thermoplastic polymer renowned for its biodegradability and absorbability. It is frequently employed in rapid prototyping applications. PLA exhibits excellent strength and stiffness at room temperature [28]. It is commonly used in the production of biodegradable medical devices like stents and implanted medication dispensers. Additionally, PLA is utilized in food packaging and disposable flatware due to its favorable properties. With its low melt temperature and user-friendly nature [29], PLA is one of the most widely used filaments for the MEX 3D printing process[30]. Table 2 provides an overview of the material properties of TPU and PLA polymers.

*Table 2: Properties of TPU and PLA*

| **Parameters** | **Values** | |
|---|---|---|
| | **TPU** | **PLA** |
| Melting point ($^oC$) | 190-210 | 200-230 |
| Density ($kg/m^3$) | 1.23 | 1.23 |
| Tensile Strength (MPa) | 26 | 52.8 |
| Bed temperature($^oC$) | 60-70 | 60-70 |
| Glass transition temperature($^oC$) | 80 | 60 |

Component design often involves managing information about materials with varying properties. One method to address this challenge is utilizing a Voxlizer-based slicing approach, enabling the manipulation of material distribution based on their respective volumes. Figure 3 illustrates the gradient interface within the investigated FGMs. Specifically, Figure 3a demonstrates a comparison between a conventional two-nozzle Multi-material AM process and the Multi-material FGM fabrication technique. This comparison highlights the distinctive capabilities of the Multi-material FGM approach in creating graded interfaces within the fabricated structures. In Figure 3b, various combinations of different materials within the FGM are displayed. The Multi-material FGM is implemented in this study using the MEX technique.

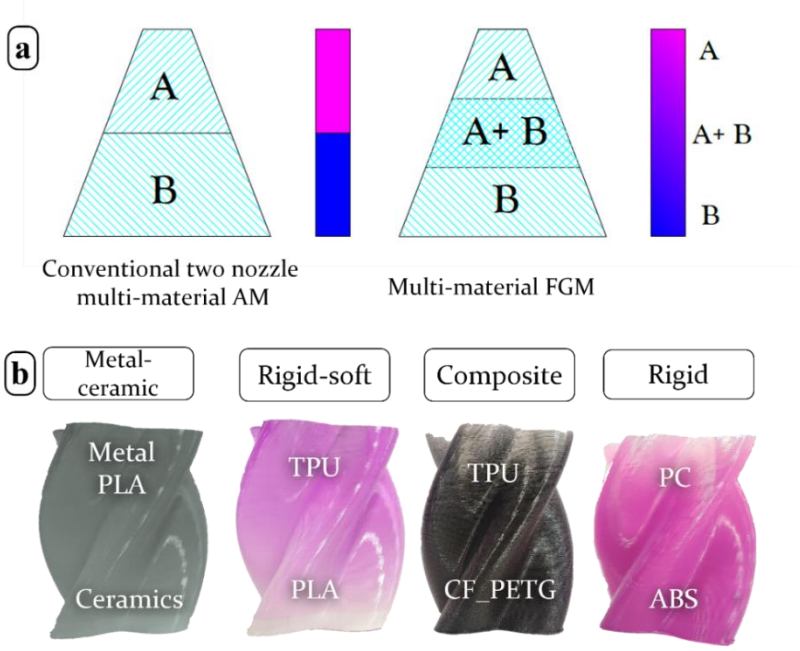


*Figure 3: Gradient transition of FGM interfaces, (a) conventional versus FGM material combination, (b) components with different material combinations* [31]

**Specimen Preparation and Fabrication**

The fatigue test specimen in this study follows the guidelines outlined in ASTM standard E606M [32], as depicted in Figure 4. The specimen dimensions, including length, width, thickness, and curvature radius, are 135 mm, 20 mm, 5 mm, and 10 mm, respectively. Figure 5 visually represents the 3D printed FGM specimen.

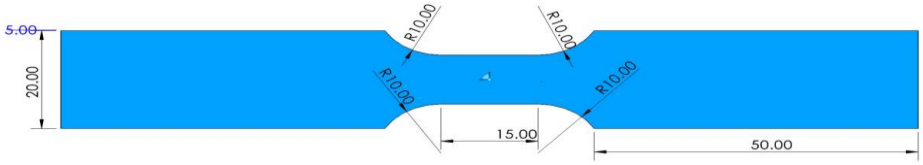


*Figure 4: Dimension of the specimen as per E606M*

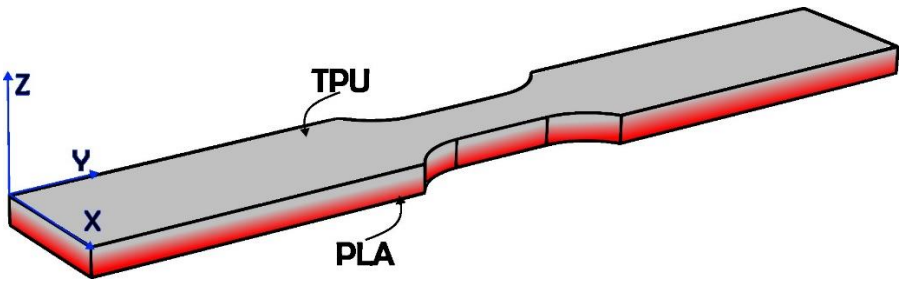


*Figure 5: 3D printed FGM specimen*

**Experimental setup**

In this study, uniaxial tensile and fatigue tests were conducted on plastics using a Testresources 810E4 [33] load frame equipped with a 15 KN load cell, following the test procedures outlined in the ASTM E606M standard. The testing setup involved a closed-loop servo-hydraulic machine of the specified model. The Newton Testware [34] interface was utilized to control and input all testing variables, such as frequency, amplitude, and average load. The testing device consisted of two grasping heads, with the upper head serving as a simple grasping mechanism and the lower head responsible for applying the load to the specimen [35]. A PID controller was employed to maintain the desired stress level during the tests. The experimental test setup is depicted in Figure 6.

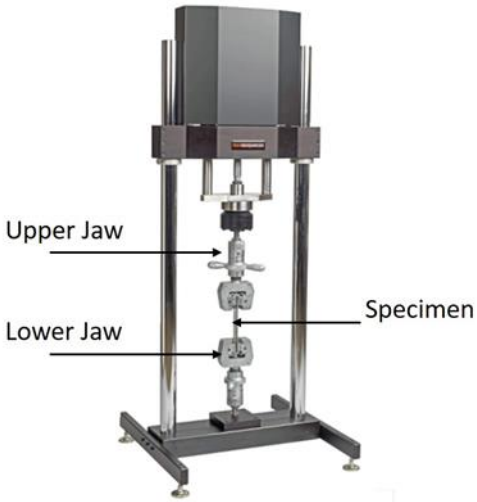


*Figure 6: Test setup*

**Tensile test**

An experimental investigation was conducted to gain a deeper understanding of the behavior of additively manufactured composite materials when subjected to different structural stresses. The study involved the use of tensile test samples, which were subjected to uniaxial loading until they reached the point of catastrophic failure within the gauge length area. The UTS values of the specimens were recorded and compared for different materials, including PLA, FGM, and TPU, all of which were printed using fixed processing parameters. The UTS values obtained for these materials are presented in Table 3. Furthermore, Figure 7 displays load-distance diagrams for PLA, TPU, and FGM specimens. Observations from the experiments indicate that the strength of the FGM material is lower than that of PLA but higher than that of TPU. These findings highlight that utilizing FGM can be an effective means of enhancing the strength of weak MEX parts.

*Table 3: UTS (MPa) of 3D printed samples*

| Sample No. | PLA | FGM | TPU |
|---|---|---|---|
| 1 | 47.46 | 30.88 | 12.50 |
| 2 | 47.63 | 30.70 | 12.16 |
| 3 | 47.31 | 31.20 | 12.64 |
| Average | 47.46 | 30.92 | 12.43 |

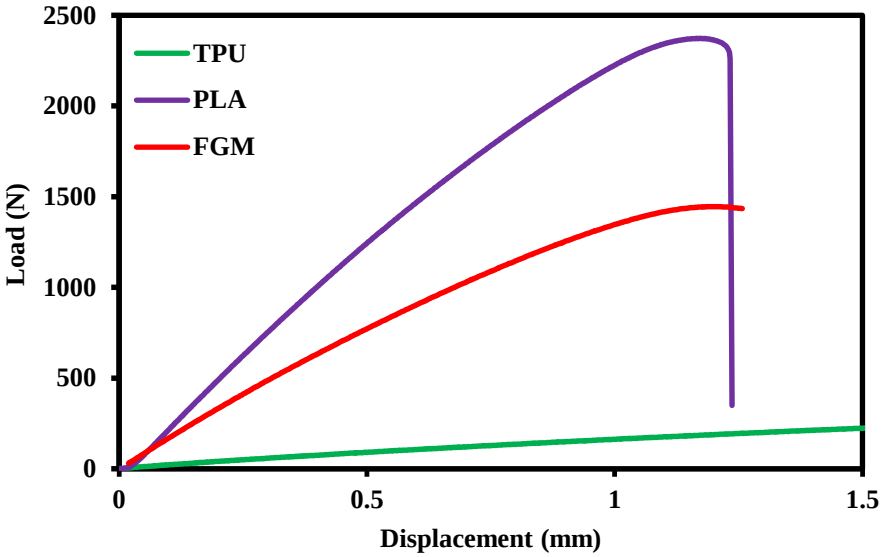


*Figure 7: Load vs Displacement*

**Fatigue test**

To assess the fatigue life of FGMs under specific conditions, a tension-based fatigue test was performed. The test involved varying parameters such as stress levels, stress ratio, and frequency. Stress levels of 80%, 60%, 40%, and 20% of the UTS were considered, with a stress ratio of 0.1. The frequency used in the test was 3 Hz. To ensure the consistency and reliability of the results, three case levels were examined, where FGM specimens were subjected to different stress levels. The test results were plotted using S-N curves. Moreover, curves are fitted with logarithmic trend line as depicted in Figure 8. The S-N curves exhibited slight variations, suggesting the presence of imperceptible anomalies such as voids, cracks, and porosity that may occur during the FGM deposition process. Notably, the specimens tested at 20% of UTS demonstrated a longer fatigue life, and the fatigue life of all samples was measured up to 140,000 cycles. Furthermore, it was observed that the specimens tested at 80% and 60% of UTS displayed characteristic behavior of low-cycle fatigue (LCF). Conversely, the specimens tested at 40% and 20% of UTS exhibited behavior associated with high-cycle fatigue (HCF). The fatigue life of the FGM specimens was found to be more sensitive to the applied load levels. These research findings hold significant importance as they provide a comprehensive analysis of how stress levels influence the material characteristics of FGM parts. Moreover, the utilization of multiple case levels ensures the reliability and repeatability of the experimental outcomes, thereby enhancing the validity and robustness of the findings.

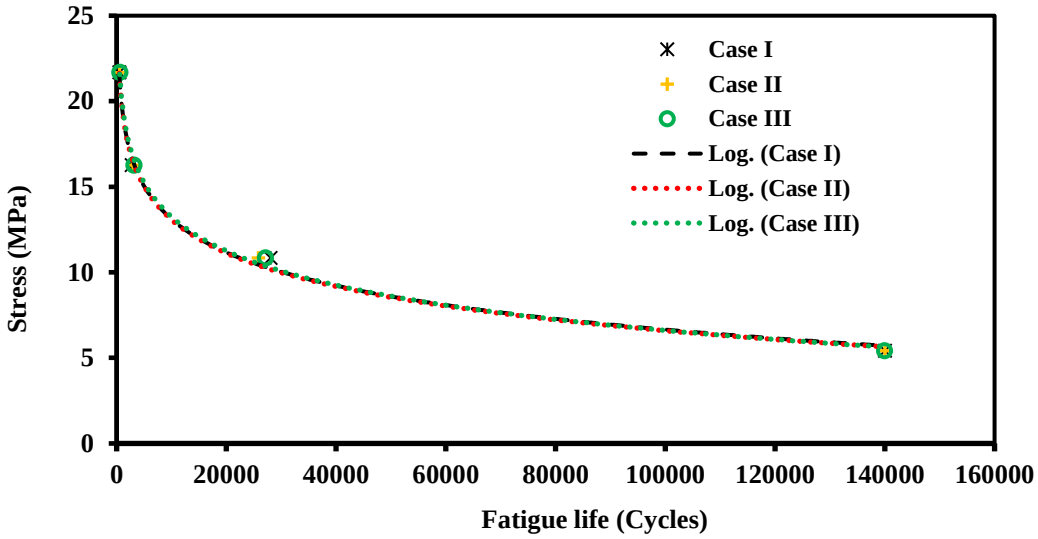


*Figure 8: S-N curve for experimental data with case I, II and III*

## The Statistical Methods of S-N Curve Models

The S-N curve plays a fundamental role in the estimation of material fatigue life. Various models have been developed to characterize experimental fatigue data subjected to constant amplitude loading and stress ratio. Researchers have employed a range of statistical models, including Basquin's Model, Weibull model [36], Sendeckyj[37] , Kim and Zhang model [13], and ANN [38], for the prediction of fatigue life. These models aim to capture the relationship between stress amplitude and the number of cycles to failure, enabling accurate fatigue life predictions for different materials and loading conditions.

### Basquin's Model

It is widely employed by researchers for the prediction of fatigue life in additively manufactured components due to its simplicity and applicability to both polymers and composite materials. In a study conducted by Andrzejewska et al. [18] fitted the S-N curve for PLA using Basquin's model for specimens fabricated through MEX and injection molding processes. Basquin's model is mathematically represented by equation 1, where $\sigma$a denotes stress amplitude, C represents the fatigue strength coefficient, b corresponds to the fatigue strength exponent, and Nf represents the number of cycles to failure. This model describes the linear relationship between the applied stress cycles and the number of cycles to failure, presented on a logarithmic scale. Basquin's model can be viewed as a power law relationship capturing the fatigue behavior of the material under consideration.

$$\Delta\sigma\, N_f^b = C \qquad (1)$$

In the Basquin's equation, $\Delta\sigma$ represents the applied peak stress, while C and b are the model fitting parameters or constants. The parameter $N_f$ corresponds to the number of cycles at failure. When plotted on logarithmic-logarithmic coordinates, the Basquin's equation yields a straight line. Equation (2), which is commonly employed for fatigue prediction, can be expressed as a linear logarithmic equation, as shown below:

$$\log \Delta\sigma + b \log N_f = \log C \qquad (2)$$

## Results and Discussion

Following the successful fabrication of novel FGM specimens through the MEX process, a comprehensive evaluation of their performance was conducted. This evaluation encompassed various mechanical tests, including uniaxial tensile testing to assess their strength under axial loading and fatigue behavior analysis under the process parameters. Additionally, a statistical model based on Basquin's model was employed to predict the fatigue life of the FGM specimens. Following the acquisition of experimental data, the fatigue life of the specimens was determined by utilizing Basquin's law equation. The values of C and b in the Basquin's model can be obtained through a process of fitting the experimental fatigue life data to the mathematical equation 1. This process involves statistical analysis and regression techniques to determine the optimal values of C and b that best represent the relationship between stress level and fatigue life are represented in Table 4.

*Table 4: Values of C and b of Basquin's relation and $R^2$ correlation*

| Samples | C | b | Experimental ($R^2$) | Basquin's Model ($R^2$) | % Difference |
|---|---|---|---|---|---|
| case I | 128.56 | 0.1722 | 0.9947 | 0.9549 | 4 |
| case II | 126.74 | 0.1738 | 0.9978 | 0.9608 | 3.7 |
| case III | 134.75 | 0.1786 | 0.9973 | 0.9608 | 3.65 |

The specimens were tested at stress levels corresponding to 80%, 60%, 40%, and 20% of the nominal UTS. The calculated fatigue life based on the experimental data was compared with the predictions obtained from the Basquin's model, and the S-N curve was plotted using a logarithmic numerical function as shown in Figure 9. In Case I, the parameters C and b in the Basquin's model were determined to be 128.56 and 0.1722, respectively as presented in Table 4. Notably, the specimens tested at the 20% UTS stress level exhibited the highest fatigue life, exceeding 140,000 cycles. However, according to Basquin's model predictions, the same stress level should yield a significantly higher number of cycles, specifically 1,727,342 cycles. The coefficient of determination ($R^2$) was used to assess the statistical variation between the dependent and independent variables. The $R^2$ value for the experimental fatigue life was determined to be 0.9947, indicating a strong correlation. Similarly, the $R^2$ value for the predicted fatigue life based on the Basquin's model was 0.9549, suggesting a good line of agreement with experimental. The percentage error between the experimental and predicted fatigue life cycles was determined to be 4% and curves are fitted with logarithmic trend line. Eventually, in Case I, it was observed that the experimental fatigue life and the predicted fatigue life cycles based on the Basquin's model exhibited some similarity. These findings hold scholarly significance as they provide insights into the comparison between experimental data and the predictions obtained from a well-known fatigue life prediction model, further contributing to the understanding of the fatigue behavior of the specimens.

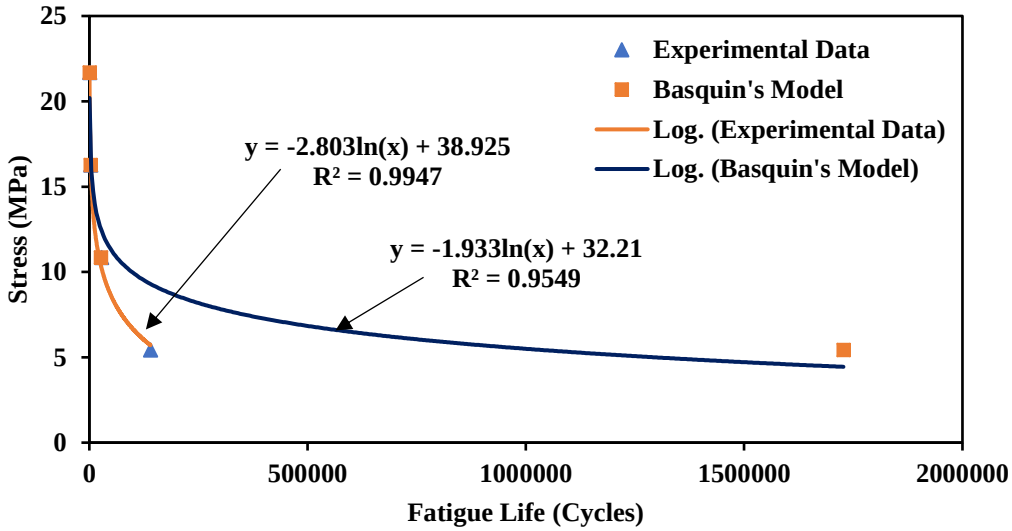


*Figure 9: S-N curve for Experimental data and Basquin's Predicted model for case I*

In Case II, the parameters C and b in the Basquin's model were determined to be 126.74 and 0.1738, respectively, as presented in Table 4. The fatigue life of the specimens tested at the 20% UTS stress level was found to be 140,000 cycles through experimental testing. Conversely, the predictions from the Basquin's model indicated a fatigue life of 1,394,213 cycles, as demonstrated by the S-N curve in Figure 10. For Case II, the $R^2$ value for the experimental fatigue life was determined to be 0.9978, indicating a high degree of correlation. Similarly, the $R^2$ value for the predicted fatigue life based on the Basquin's model was 0.960849, suggesting a reasonably within the expected region of the variation. The percentage error between the experimental and predicted fatigue life cycles was found to be 3.7% and curves are fitted with logarithmic trend line.

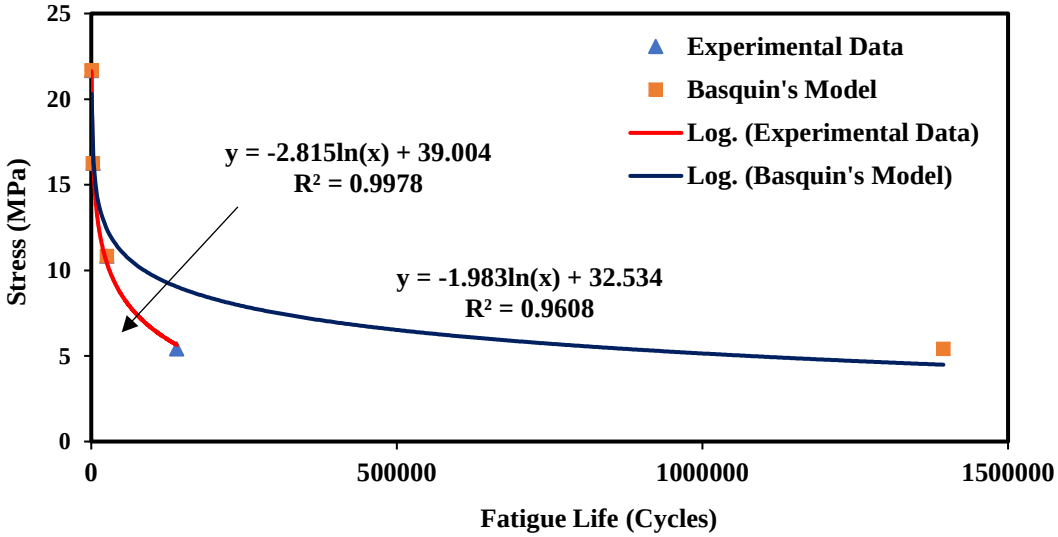


*Figure 10: S-N curve for Experimental data and Basquin's Predicted model for case II*

In Case III, the Basquin's model parameters were calculated to be C = 134.75 and b = 0.1786, as presented in Table 4. The experimental testing revealed a fatigue life of 140,000 cycles for the specimens subjected to a stress level of 20% UTS. However, Basquin's model predicted a fatigue life of 1,315,760 cycles, Moreover, curves are fitted with logarithmic trend line as depicted in Figure 11. For Case III, the $R^2$ value for the experimental fatigue life was found to be 0.9973, indicating a strong correlation between the measured and observed data. Similarly, the $R^2$ value for the predicted fatigue life based on the Basquin's model was 0.9608, suggesting a reasonably consistent with the experimental data. The percentage error between the experimental and predicted fatigue life cycles was calculated to be 3.5%.

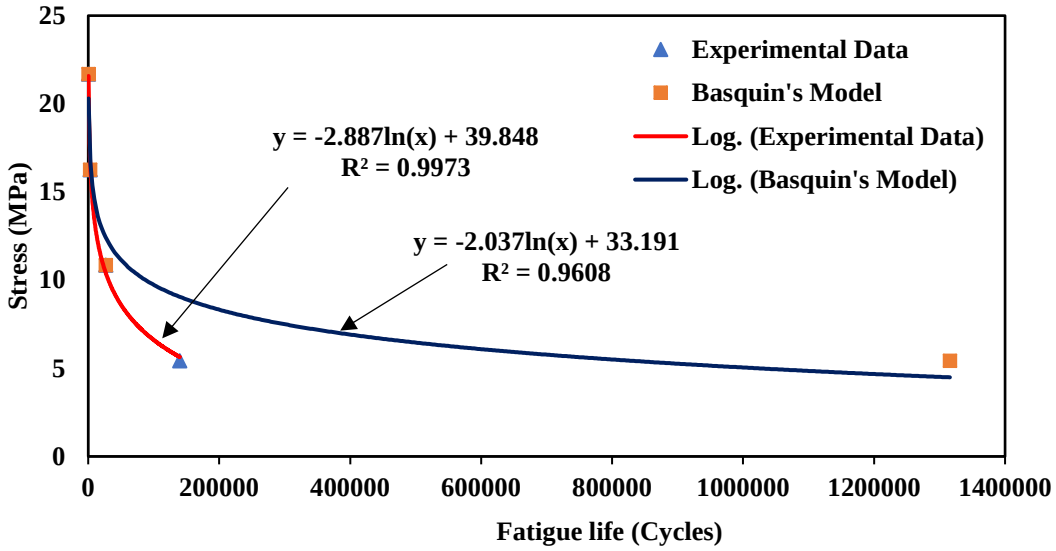


*Figure 11: S-N curve for Experimental data and Basquin's Predicted model for Case III*

Comparing Case I, Case II, and Case III, all three cases demonstrated high $R^2$ values, indicating significant correlations between the experimental and predicted fatigue life. Furthermore, the percentage errors for all cases were relatively low, with Case I having a percentage error of 4%, Case II having a percentage error of 3.7%, and Case III having a percentage error of 3.5%. These findings illustrate the effectiveness of the Basquin's model, with the calculated values of C and b, in predicting the fatigue life of the FGM specimens across different stress levels. In summary, all three cases exhibited strong correlations between the experimental and predicted fatigue life. The Basquin's model, with the calculated parameters, accurately predicted the fatigue behavior of the FGM specimens tested at various stress levels. These findings contribute to the understanding of fatigue characteristics in FGM materials and highlight the reliability of the Basquin's model in estimating fatigue life under different stress conditions.

## Validating Basquin's Model for Fatigue Life Prediction in Additively Manufactured Polymeric FGM Materials

To validate the applicability of the Basquin's model to FGM materials, a comprehensive study was conducted involving three different stress levels: 90%, 70%, and 50% of the UTS. The research approach involved initially predicting the fatigue life using the Basquin's model and estimating the corresponding values of C and b. Subsequently, experimental testing was conducted to obtain the

actual fatigue life data. The first step in the validation process was to apply the Basquin's model to predict the fatigue life of the FGM specimens at aforementioned stress levels. Based on this initial prediction, the values of C and b were calculated for each stress level. These values served as crucial parameters for further analysis. Next, experimental fatigue tests were conducted on the FGM specimens under the specified stress levels. The obtained experimental data was then compared to the predictions made by Basquin's model. To quantify the correlation between the experimental and predicted fatigue lives, a power function was utilized to plot the S-N curve and fit it to the experimental data. The $R^2$ was then computed, Moreover, curves are fitted with power trend line as depicted in Figure 12.

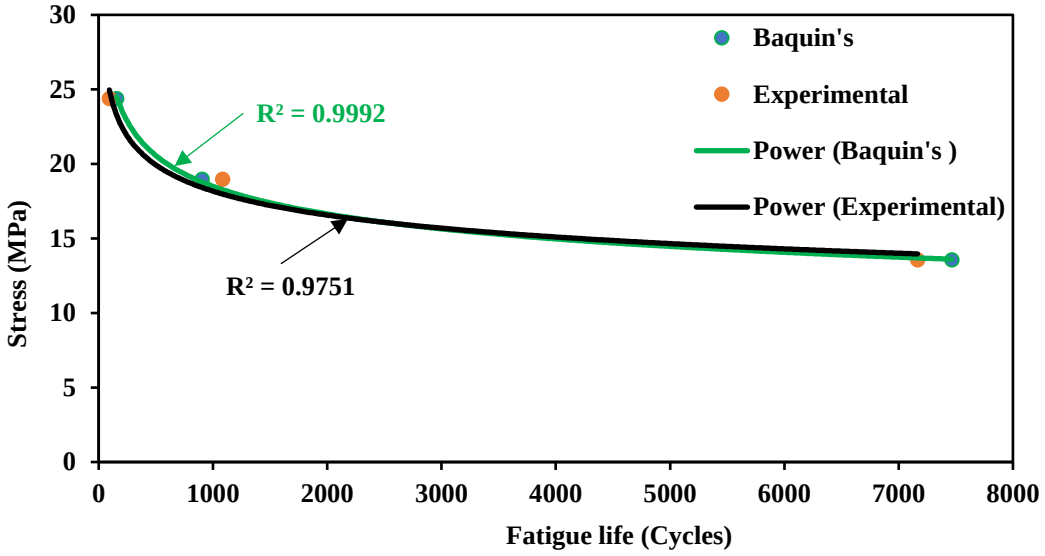


*Figure 12: Comparison of Basquin's model with experimental data*

The results of the validation study demonstrated a remarkable agreement between Basquin's model predictions and the experimental fatigue life data. The $R^2$ value for the Basquin's model was calculated to be 0.9991, indicating a strong correlation between the predicted and experimental fatigue lives. This high $R^2$ value demonstrates the excellent agreement between the model's predictions and the actual experimental data. Similarly, the experimental $R^2$ value was determined to be 0.9763, providing further evidence of the consistent relationship between the experimental results and the predicted values. These findings, as presented in Table 5, confirm the reliability and accuracy of the Basquin's model in predicting fatigue life.

*Table 5: Values of C and b of Basquin's relation and R2 correlation*

| C | b | Experimental ($R^2$) | Basquin's Model ($R^2$) | % Difference |
|---|---|---|---|---|
| 129.2 | 0.1749 | 0.9763 | 0.9953 | 1.90% |

The small percentage error difference of 1.9% between the Basquin's model predictions and the experimental results confirmed the suitability and accuracy of the model for predicting the fatigue life of FGM materials subjected to different stress levels. These findings provide strong evidence that the Basquin's model is a reliable and effective tool for assessing the fatigue behavior of FGM

materials. In conclusion, the validation study demonstrated that the Basquin's model, with the calculated values of C and b, provided an excellent fit for predicting the fatigue life of FGM specimens under various stress levels. The high $R^2$ values and low percentage error difference underscores the robustness and accuracy of the model, validating its suitability for assessing the fatigue performance of FGM materials in engineering applications.

## Conclusions

This article presents a concise overview of an experimental study conducted on FGM specimens manufactured using the MEX process. The study focuses on the characterization of tensile properties and fatigue behavior, with particular emphasis on predicting fatigue life. The main findings of this research can be summarized as follows:

- FGMs exhibited promising mechanical properties in terms of tensile strength and fatigue behavior.
- FGMs exhibited intermediate strength between PLA and TPU, suggesting their potential for strengthening weak MEX components.
- Fatigue testing at different stress levels demonstrated that FGM specimens exhibited both low-cycle fatigue and high-cycle fatigue behavior.
- The fatigue life of FGM specimens was more sensitive to load levels, with longer fatigue life observed at lower stress levels.
- Basquin's model demonstrated strong correlation and reliability in predicting fatigue life for FGM.
- The comprehensive analysis of stress levels' influence on FGM material characteristics provides valuable insights for designing and optimizing FGM parts in various applications.

## References


[1] S. Hasanov *et al.*, "Review on Additive Manufacturing of Multi-Material Parts: Progress and Challenges," *Journal of Manufacturing and Materials Processing 2022, Vol. 6, Page 4*, vol. 6, no. 1, p. 4, Dec. 2021, doi: 10.3390/JMMP6010004.

[2] "I. Fidan, M. Norris, M. Rajeshirke, O. Huseynov, S. Alkunte, J. K. Dasari, Z. Zhang, Non-traditional Delivery of Hands-on Manufacturing Courses, Proceedings of the ASEE2022, Minneapolis, Minnesota, June 26-29, 2022, https://peer.asee.org/40950".

[3] M. Alshaikh, A. I. Fidan, M. A. Ali, and I. Fidan, "Investigation of the Impact of Power Consumption, Surface Roughness, and Part Complexity in Stereolithography and Fused Filament Fabrication," *The International Journal of Advanced Manufacturing Technology*, 2023, doi: 10.1007/s00170-023-11279-3.

[4] O. Huseynov, S. Hasanov, and I. Fidan, "Influence of the matrix material on the thermal properties of the short carbon fiber reinforced polymer composites manufactured by material extrusion," *J Manuf Process*, vol. 92, pp. 521–533, Apr. 2023, doi: 10.1016/J.JMAPRO.2023.02.055.

[5] M. Rajeshirke, I. Fidan, A. Gupta, and K. Mäntyjärvi, "Fatigue Analysis of Short Carbon Fiber Reinforced Composite Components Manufactured Using Fiber-Reinforced Additive Manufacturing," 2022, doi: 10.26153/TSW/44139.

[6] I. Fidan *et al.*, "Recent Inventions in Additive Manufacturing: Holistic Review," *Inventions 2023, Vol. 8, Page 103*, vol. 8, no. 4, p. 103, Aug. 2023, doi: 10.3390/INVENTIONS8040103.

[7] I. Fidan *et al.*, "The trends and challenges of fiber reinforced additive manufacturing," *International Journal of Advanced Manufacturing Technology*, vol. 102, no. 5–8, pp. 1801–1818, Jun. 2019, doi: 10.1007/S00170-018-03269-7/METRICS.

[8] S. Hasanov, A. Gupta, A. Nasirov, and I. Fidan, "Mechanical characterization of functionally graded materials produced by the fused filament fabrication process," *J Manuf Process*, vol. 58, pp. 923–935, Oct. 2020, doi: 10.1016/J.JMAPRO.2020.09.011.

[9] S. Hasanov, A. Gupta, F. Alifui-Segbaya, and I. Fidan, "Hierarchical homogenization and experimental evaluation of functionally graded materials manufactured by the fused filament fabrication process," *Compos Struct*, vol. 275, p. 114488, Nov. 2021, doi: 10.1016/J.COMPSTRUCT.2021.114488.

[10] S. Hasanov, "NUMERICAL MODELING AND EXPERIMENTAL CHARACTERIZATION OF FUNCTIONALLY GRADED MATERIALS MANUFACTURED BY THE FUSED FILAMENT FABRICATION PROCESS," 2021.

[11] S. Alkunte, I. Fidan, and S. Hasanov, "Experimental Analysis of Functionally Graded Materials produced by Fused Filament Fabrication," 2022, doi: 10.26153/TSW/44144.

[12] G. Dolzyk and S. Jung, "Tensile and Fatigue Analysis of 3D-Printed Polyethylene Terephthalate Glycol," *Journal of Failure Analysis and Prevention*, vol. 19, no. 2, pp. 511–518, Apr. 2019, doi: 10.1007/S11668-019-00631-Z/METRICS.

[13] I. Burhan and H. S. Kim, "S-N Curve Models for Composite Materials Characterisation: An Evaluative Review," *Journal of Composites Science 2018, Vol. 2, Page 38*, vol. 2, no. 3, p. 38, Jul. 2018, doi: 10.3390/JCS2030038.

[14] H. S. Kim and J. Zhang, "Fatigue Damage and Life Prediction of Glass/Vinyl Ester Composites," *http://dx.doi.org/10.1177/073168401772678959*, vol. 20, no. 10, pp. 834–848, Jul. 2001, doi: 10.1177/073168401772678959.

[15] L. Safai, J. S. Cuellar, G. Smit, and A. A. Zadpoor, "A review of the fatigue behavior of 3D printed polymers," *Addit Manuf*, vol. 28, pp. 87–97, Aug. 2019, doi: 10.1016/J.ADDMA.2019.03.023.

[16] "ISO/ASTM 52900:2015 - Additive manufacturing - General principles - Terminology." https://webstore.ansi.org/standards/iso/isoastm529002015?msclkid=5b813adbfa9e1de2e19a5eb06482e100&utm_source=bing&utm_medium=cpc&utm_campaign=Campaign%20%231&utm_term=ISO%20ASTM%2052900&utm_content=ISO-20K%2B (accessed May 21, 2023).

[17] O. Basquin, "The exponential law of endurance tests".

[18] A. Andrzejewska, L. Pejkowski, and T. Topoliński, "Tensile and Fatigue Behavior of Additive Manufactured Polylactide," *https://home.liebertpub.com/3dp*, vol. 6, no. 5, pp. 272–280, Oct. 2019, doi: 10.1089/3DP.2017.0154.

[19] H. Eskandari and H. S. Kim, "A Theory for Mathematical Framework and Fatigue Damage Function for the S-N Plane," *ASTM Special Technical Publication*, vol. STP 1598, pp. 299–336, Apr. 2017, doi: 10.1520/STP159820150099.

[20] H. Si, Z. Zhang, O. Huseynov, I. Fidan, S. R. Hasan, and M. Mahmoud, "Machine Learning-Based Investigation of the 3D Printer Cooling Effect on Print Quality in Fused Filament Fabrication: A Cybersecurity Perspective," *Inventions 2023, Vol. 8, Page 24*, vol. 8, no. 1, p. 24, Jan. 2023, doi: 10.3390/INVENTIONS8010024.

[21] A. D. Pertuz, S. Díaz-Cardona, and O. A. González-Estrada, "Static and fatigue behaviour of continuous fibre reinforced thermoplastic composites manufactured by fused deposition modelling technique," *Int J Fatigue*, vol. 130, p. 105275, Jan. 2020, doi: 10.1016/J.IJFATIGUE.2019.105275.

[22] M. Brčić, S. Kršćanski, and J. Brnić, "Rotating Bending Fatigue Analysis of Printed Specimens from Assorted Polymer Materials," *Polymers 2021, Vol. 13, Page 1020*, vol. 13, no. 7, p. 1020, Mar. 2021, doi: 10.3390/POLYM13071020.

[23] S. Ghods, R. Schur, A. Montelione, R. Schleusener, D. D. Arola, and M. Ramulu, "Importance of Build Design Parameters to the Fatigue Strength of Ti6Al4V in Electron Beam Melting Additive Manufacturing," *Materials (Basel)*, vol. 15, no. 16, Aug. 2022, doi: 10.3390/MA15165617.

[24] P. G. Mu, X. P. Wan, and M. Y. Zhao, "A new S-N curve model of fiber reinforced plastic composite," *Key Eng Mater*, vol. 462–463, pp. 484–488, 2011, doi: 10.4028/WWW.SCIENTIFIC.NET/KEM.462-463.484.

[25] S. Hassanifard and K. Behdinan, "Effects of voids and raster orientations on fatigue life of notched additively manufactured PLA components," *International Journal of Advanced Manufacturing Technology*, vol. 120, no. 9–10, pp. 6241–6250, Jun. 2022, doi: 10.1007/S00170-022-09169-1/METRICS.

[26] "Suryakant AS, Gajjal SY, Mahajan DA. Contact Stress Analysis for'Gear'to Optimize Mass using CAE Techniques. Int. J. Sci. Eng. Technol. Res. 2014;3:3491-5.".

[27] M. Norris, I. Fidan, and M. Allen, "Rheological Characterization of Room Temperature Powder Metal Paste for Extruded Material Modeling," 2022, doi: 10.26153/TSW/44186.

[28] R. Buchanan, J. Kumar Dasari, I. Fidan, M. Allen, and I. Bhattacharya, "Knowledge Base Development for Mechanical Properties and Energy Consumption of Iron-PLA Composite Filaments in Additive Manufacturing," 2022, doi: 10.26153/TSW/44539.

[29] O. Huseynov and I. Fidan, "INFLUENCE OF THE DIFFERENT MATRIX MATERIALS ON THE THERMAL PROPERTIES OF SHORT CARBON FIBER REINFORCED COMPOSITES MANUFACTURED BY FUSED FILAMENT FABRICATION".

[30] S. Alkunte, M. Rajeshirke, I. Fidan, and S. Hasanov, "Performance evaluation of fatigue behavior in extrusion-based functionally graded materials," *International Journal of Advanced Manufacturing Technology*, vol. 128, no. 1, pp. 863–875, Jul. 2023, doi: 10.1007/S00170-023-11922-Z/METRICS.

[31] S. Hasanov, A. Gupta, A. Nasirov, and I. Fidan, "Mechanical characterization of functionally graded materials produced by the fused filament fabrication process," *J Manuf Process*, vol. 58, pp. 923–935, Oct. 2020, doi: 10.1016/J.JMAPRO.2020.09.011.

[32] "compass." https://compass.astm.org/document/?contentCode=ASTM%7CE0606_E0606M-21%7Cen-US&proxycl=https%3A%2F%2Fsecure.astm.org&fromLogin=true (accessed May 21, 2023).

[33] "Dynamic and Fatigue Test Machines." https://www.testresources.net/test-machines/dynamic-fatigue-test-machines/ (accessed May 21, 2023).

[34] "Newton Test Machine Controller." https://www.testresources.net/test-machines/newton-test-machine-controller/ (accessed May 21, 2023).

[35] M. Rajeshirke, S. Alkunte, O. Huseynov, and I. Fidan, "Fatigue analysis of additively manufactured short carbon fiber-reinforced PETG Components," *International Journal of Advanced Manufacturing Technology*, pp. 1–18, Aug. 2023, doi: 10.1007/S00170-023-12107-4/METRICS.

[36] S. Sire, P. D. Toasa Caiza, B. Espion, and M. Ragueneau, "Contribution to the study of the influence of the stress ratio on the high cycle fatigue behaviour of riveted joints," *Fatigue Fract Eng Mater Struct*, vol. 43, no. 12, pp. 3027–3036, Dec. 2020, doi: 10.1111/FFE.13324.

[37] A. K. Vanhari, E. Fagan, and J. Goggins, "A novel estimation method for fitting fatigue data in the composite wearout model," *Compos Struct*, vol. 287, p. 115384, May 2022, doi: 10.1016/J.COMPSTRUCT.2022.115384.

[38] H. Si, Z. Zhang, O. Huseynov, I. Fidan, S. R. Hasan, and M. Mahmoud, "Machine Learning-Based Investigation of the 3D Printer Cooling Effect on Print Quality in Fused Filament Fabrication: A Cybersecurity Perspective," *Inventions 2023, Vol. 8, Page 24*, vol. 8, no. 1, p. 24, Jan. 2023, doi: 10.3390/INVENTIONS8010024.

## Statements & Declarations

**Funding:** This research project is based upon work supported by the Center for Manufacturing Research (CMR) and Mechanical Engineering Department. This support is greatly appreciated by the authors.

**Author Contributions:** All authors contributed to various portions of the research project, mostly, however, by Ismail Fidan. Methodology, experimentation, and analysis were mostly done by Suhas Alkunte and Mithila Rajeshirke. The initial draft was written by Suhas Alkunte and Mithila Rajeshirke; revised and finalized by Ismail Fidan. All authors read and approved the final manuscript.

**Conflicts of Interest:** The authors declare no relevant financial or non-financial interests.